Intelligent Vehicles Symposium 2006, June 13-15, 2006, Tokyo, Japan

3-13

Parking Slot Markings Recognition for Automatic Parking Assist System

Ho Gi Jung, Dong Suk Kim, Pal Joo Yoon

Central R&D Center
MANDO Corporation
Yongin-Si 446-901, Koera

Jaihie Kim

School of Electrical and Electronic Engineering
Yonsei University
Seoul 120-749, Korea

Abstract

This paper describes a monocular vision based parking-slot-markings recognition algorithm, which is used to automate the target position selection of automatic parking assist system. Peak-pair detection and clustering in Hough space recognize marking lines. Specially, one-dimensional filter in Hough space is designed to utilize a priori knowledge about the characteristics of marking lines in bird's eye view edge image. Modified distance between point and line-segment is used to distinguish guideline from recognized marking line-segments. Once the guideline is successfully recognized, T-shape template matching easily recognizes dividing marking line-segments. Experiments show that proposed algorithm successfully recognizes parking slots even when adjacent vehicles occlude parking-slot-markings severely.

1. Introduction

Semi-automatic or full automatic parking system is one of the most interesting driver assistant systems [1]. J. D. Power's 2001 Emerging Technology Study shows that 66% of consumers are likely to purchase parking aid [2]. Almost upper class and middle-class vehicles are equipped with ultrasonic-based parking aid systems. Recently, car manufacturers and component manufacturers are developing semi-automatic parking assistant system, which automates steering maneuver during parking operation [3]-[6].

Automatic parking system consists of six components: environment recognition, path generation, pose estimation, path tracking controller, active steering/braking system, and HMI (Human Machine Interface). Semi-automatic parking system leaves braking maneuver, i.e. speed control, to driver's responsibility. Although current systems generally use range sensors such as ultrasonic [5], laser scanner [7] as an environment recognition sensor, vision systems are expected to be the major sensor of upcoming systems.

Vision systems for automatic parking system can be categorized into 3 approaches according to the kind of recognized objects. First approach recognizes adjacent vehicles as the boundary of available parking slot [8]-[10]. Nico Kaempchen developed stereo vision based pose estimation of parked vehicles, which used feature based stereo algorithm, template matching algorithm on depth map and 3D fitting to the planar surface model of vehicle by ICP (Interactive Closest Point) algorithm [10]. Aisin Seiki's next generation developed motion stereo based IVR (Intermediate View Reconstruction) to provide a virtual rendered image from an optimistic viewpoint [8]-[9]. Second approach recognizes only parking slot markings [11]. Jin Xu developed color vision based localization of parking site marking, which used color segmentation based on RCE neural network, contour extraction based on least square method and inverse perspective transformation [11]. Finally, third approach recognizes both parking slot markings and adjacent vehicles [12]-[13]. My previous work uses stereo vision based free parking site recognition, which reduces search range by using adjacent vehicle's depth map, then recognizes parking slot markings by rectangular template matching [12]-[13].

Proposed method in this paper can be categorized into second approach. We have been trying to develop economically practical vision solution for semi-automatic parking assist system. It is supposed that binocular stereo vision and motion stereo vision are too expensive to be adopted by the first mass-produced parking systems. Furthermore, monocular

vision system, which recognizes only parking slot marking, should be able to manage occlusions by adjacent vehicles.

Proposed method consists of six phases: construction of the bird's eye view edge image of input image captured with wide-angle lens, Hough transform of edge image, marking line recognition by peak pair detection, marking line-segment recognition, guideline recognition using modified distance between a point and a line-segment, and dividing marking line-segment recognition. The peak pair detection uses an assumption that one marking line-segment becomes a parallel line-segment pair distant by fixed width in edge image and it forms a characteristic pattern in Hough space. One-dimensional filter incorporating such a priori knowledge successfully detects marking line-segment. It shares many things with newly developed approaches that focus on the geometrical structure of peaks in Hough space [14]-[16]. Modified distance between a point and a line-segment is designed to reflect the geometrical structure of parking slot markings. Experiments show that the proposed method can successfully recognize parking slot markings in spite of severe occlusion by adjacent vehicles.

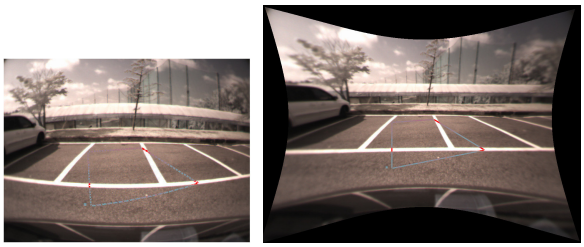

(a) Input image (b) Undistorted image

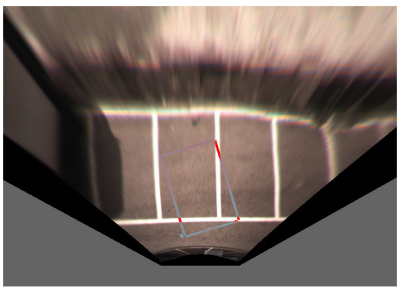

(c) Bird's eye view image

Fig. 1. Construction of bird's eye view image

2. Hough Transform

2.1 Bird's Eye View Edge Image

Rear-view image captured with wide-angle lens is transformed into bird's eye view image. First, input image is undistorted by radial lens distortion model [17]. Then, undistorted image is transformed into bird's eye view image with homography, which defines one-to-one relation between two coordinate systems [18]. In our system, camera is supposed to have constant height and tilt angle. Therefore, homography is measured once during camera calibration procedure [18]. Fig. 1 shows the bird's eye view image of input image.

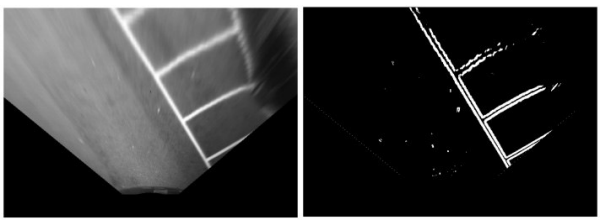

Fig. 2. Bird's eye view image and edge image

$$E(x,y) = \left| \sum_{i=-1}^{1} \sum_{j=-1}^{1} Sobel_{vertical}(i,j) \cdot B(x+i,y+j) \right| + \left| \sum_{i=-1}^{1} \sum_{j=-1}^{1} Sobel_{horizontal}(i,j) \cdot B(x+i,y+j) \right| \quad (1)$$

Edge image is generated from bird's eye view image using Sobel edge detector. Each pixel of the edge image is the summation of Sobel horizontal mask application and Sobel vertical mask application like (1). In (1), *E(x,y)* denotes a pixel value of the edge image and *B(x,y)* denotes a pixel value of the bird's eye view image. Resultant edge image is a binary image acquired by applying a certain threshold to the calculated *E(x,y)*. Fig. 2 shows a bird's eye view image and resultant edge image.

2.2 Hough Transform of Edge Image

Parking slot Marking consists of several marking line-segments, each of which appears as a parallel line-segment pair with fixed distance in the edge

image. The line-segment pair is corresponding to the both side borders of a marking line-segment. It is noticeable that a parallel line-segment pair with fixed distance forms a characteristic pattern in Hough space. In other words, two peaks in Hough space corresponding to the line-segment pair are supposed to have almost the same coordinates in orientation axis and be distant from each other with the fixed distance in the distance axis of Hough space. Furthermore, two peaks are supposed to have the same height.

Hough Transform is one of the most popular methods for the detection of line in binary image. A pixel (x,y) in binary image is transformed into a set of parameters (θ,d), each of which is corresponding to a line passing the pixel in binary image. If all pixels in a binary image are transformed into corresponding parameter sets and contributions of the parameter sets are accumulated in Hough space, a line in binary image forms a peak in Hough space. Therefore, peak detection in Hough space can recognize lines in binary image [19].

In general, Hough transform uses normal vector direction φ and distance ρ as Hough space axes. In this research, for the sake of easier interface with another components of vision system, somewhat different axes are used: orientation angle θ instead of normal vector direction φ, signed distance d instead of positive distance ρ. With the new axes, pairing two lines having different signs of intersection become to have the same orientation with each other. It is contrast to the general axes, with which pairing lines passing the upside and downside of the origin have different normal vector direction with the displacement of π. With the new axes, the distance between two lines can be calculated simply by subtracting their signed distances d. In the case of the general axes, calculating distance between lines should consider the range of normal vector directions. Equation (2) shows the definition of θ and d.

$$\begin{aligned} y &= a \cdot x + b = \tan\theta \cdot x + b \\ d &= b \cdot |\cos\theta| \end{aligned} \tag{2}$$

If there are many lines in edge image, there will be corresponding peaks in Hough space. Because the height of a peak in Hough space depends on the length of corresponding line-segment, it is impossible to detect valid peaks with a fixed threshold. Furthermore, because contributions from several lines are overlapped in Hough space, interference between peaks is unavoidable [20]. To overcome the difficulties, various methods have been developed. Among them, methods using 'butterfly pattern' provide consequent mathematical understanding about Hough transform and show robust detection performance [19]. The expression 'butterfly pattern' is from the fact that the distribution around a peak looks like a butterfly. Using butterfly pattern, it is also possible to detect the start point, end point and thickness of a line-segment. However, because analysing distributions around all peaks requires enormous computational load and time, such kind of methods are hard to be applied to real-time applications.

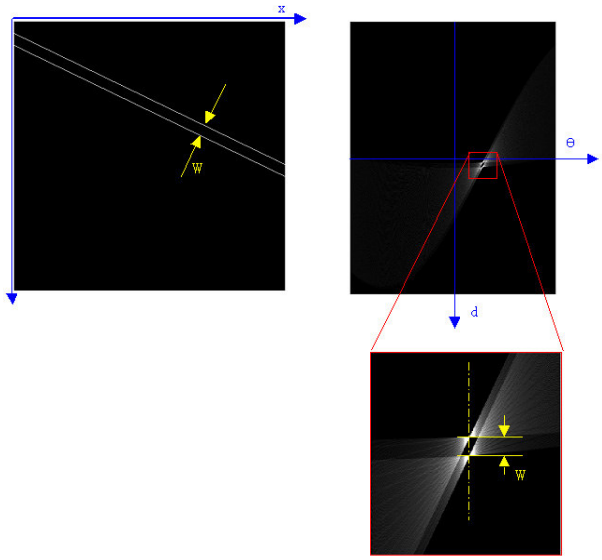

(a) Edge image (b) Hough space

Fig. 3. Hough transform of a parallel line pair

To overcome the drawback of methods using butterfly pattern, distribution pattern specified for parallel line-segment pair is devised. It is found that grasping the characteristics of distribution pattern can reduce search range, consequently eliminates the effect of noise and improves the computational speed. Fig. 3 shows that a parallel line-segment pair

with fixed distance W is transformed into characteristic distribution pattern in Hough space. Two peaks corresponding to respective line-segments have the same θ value and are distant by W in d axis. Furthermore, the heights of peaks are all the same and there is a deep valley between the peaks.

3. Marking Line-segment Recognition

3.1. Marking Line Recognition

1D(one-dimensional) filtering and clustering in Hough space are developed to detect peak pairs, whose two peaks have the same θ value and fixed between-distance W in d axis in Hough space. There is no general characteristic of the peak pair in θ axis direction, because the wing-width and starting-point of butterfly pattern are various depending on the location and length of line-segment. Therefore, 1D filtering in d axis direction, which incorporates a priori knowledge about the peak pair in Hough space, detects candidates of peak pair. Consecutively, candidate clusters are detected by morphological dilation and connected component searching. It is certified that the centroid of each cluster is a good estimate of a marking line parameter corresponding to the peak pair.

Equation (3) and Fig. 4 show the structure of designed 1D filter. $HS(\Theta,d)$ is the value of a Hough space element at (Θ,d). The designed filter is based on the fact that if the investigated coordinates in Hough space is (Θ,d) and it is a valid marking line-segment, $HS(\Theta,d)$, $HS(\Theta,d\text{-}W)$ and $HS(\Theta,d+W)$ are supposed to be valleys, simultaneously, $HS(\Theta,d\text{-}W/2)$ and $HS(\Theta,d+W/2)$ are supposed to be peaks. P_A, P_B denotes respectively each value of two peakness-testing coordinates. To reduce the effect of assumed width W and improve detection robustness, peakness-testing finds a maximum value within a predefined range in d axis direction. $S(\Theta,d)$ is the application result of the designed filter. Only when $S(\Theta,d)$ is positive, $L(\Theta,d)$ is defined as a likelihood ranging between 0~1. When the valley values are all zeros, $S(\Theta,d)$ has its maximum value, P_A+P_B. Therefore, Dividing $S(\Theta,d)$ by P_A+P_B normalizes $L(\Theta,d)$ for it to be between 0~1. In addition, multiplying the ratio, minimum peak value over maximum peak value, encourages the case when the two peaks have the same heights. If $L(\Theta,d)$ is greater than the threshold $\Theta_{dual\ peak}$, the coordinates (Θ,d) in Hough space becomes a candidate of marking line-segment.

$$S(\theta,d) = -HS(\theta,d-W) + P_A - HS(\theta,d) + P_B - HS(\theta,d+W)$$

$$\begin{aligned} P_A &= \max_{i=-1\sim1} HS(\theta, d-\tfrac{W}{2}-i) \\ P_B &= \max_{i=-1\sim1} HS(\theta, d+\tfrac{W}{2}-i) \end{aligned} \qquad (3)$$

$$L(\theta,d) = \begin{cases} \dfrac{\min(P_A,P_B)}{\max(P_A,P_B)} \cdot \dfrac{S(\theta,d)}{P_A+P_B} & ,S(\theta,d) > 0 \\ 0 & ,S(\theta,d) \le 0 \end{cases}$$

$$C(\theta,d) = \begin{cases} 1 & ,L(\theta,d) > \theta_{dual\ peak} \\ 0 & ,L(\theta,d) \le \theta_{dual\ peak} \end{cases}$$

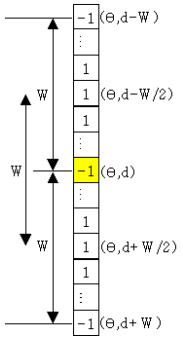

Fig. 4. Structure of 1D filter

Although almost candidates belonging to a line-segment form a cluster in Hough space, there exist some candidates that are not connected to the cluster depending on the thickness and length of the line-segment. To compensate the drawback of binarization, dilation using 5x5 rectangular kernel is used to robustly detect candidate clusters. Fig. 5(a) shows detected candidate clusters and their centroids. Fig. 5(b) and (c) show overlaid lines designated by detected centroids in edge image and undistorted image. It certifies that the designed 1D filter can

successfully detect peak pairs and the centroids of candidate clusters are good estimates of line parameters.

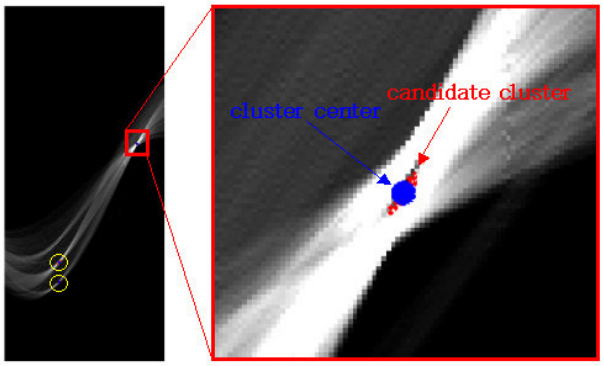

(a) Detected peak pair

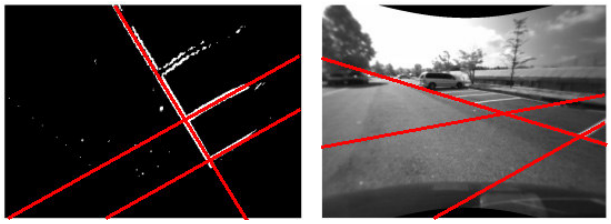

(b) In edge image (c) In undistorted image

Fig. 5. Recognized marking lines

3.2. Line-segment Recognition

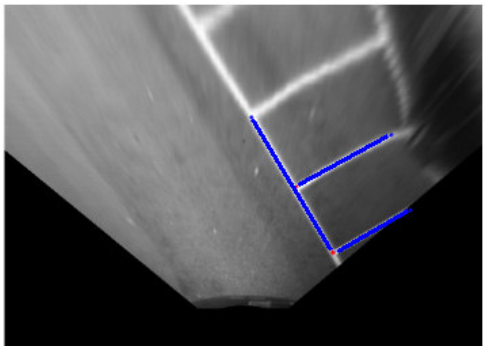

Fig. 6. Recognized marking line-segments

Marking line-segment is recognized as a section of detected marking line, which satisfies the condition of marking line-segment. In this case, the priori knowledge used in peak pair detection is used again. In other words, a marking line-segment consists of two parallel line-segments with fixed distance W in edge image. Introduction of hysteresis in the procedure improves system's robustness against noise. To determine the start-point, likelihood should be greater than starting-checking threshold continuously for $W/2$. Inversely, to determine the stop-point, likelihood should be less than stopping-checking threshold for $W/2$. Therefore, thresholding with hysteresis prevents possibilities that short-term variation of likelihood disturbs the recognition of start-point and stop-point.

4. Parking Slot Marking Recognition

4.1. Guideline Recognition

Among the recognized marking line-segments of parking slot markings, guideline is selected using an assumption that it is near from the camera and likely to be normal to the gaze direction. Guideline is the most important line-segment as the reference of parking slot recognition, because it is the border between parking slots and roadway.

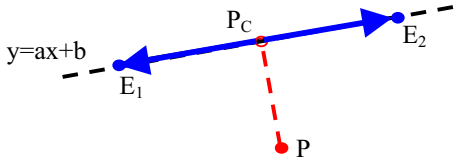

(a) When **Pc** is in the line-segment.

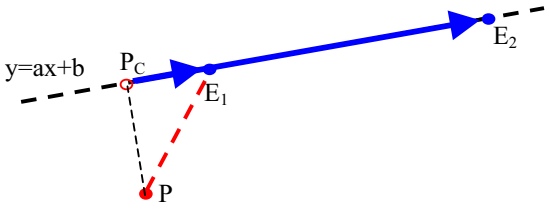

(b) When **Pc** is out of the line-segment.

Fig. 7. Distance between a point and a line-segment

In accordance with the foot of a perpendicular, distance between a point and a line-segment is defined as one of two values: distance between the point and a line extending the line-segment, minimum of two distances between the point and the two endpoints of the line-segment. In other words, if

the foot of a perpendicular is in the line-segment as shown in Fig. 7(a), distance between the point and the line-segment is defined as distance between the point and the foot of a perpendicular. In opposite case as shown in Fig. 7(b), minimum of two distances between the point and two endpoints of line-segment is selected. The foot of a perpendicular $\mathbf{P_C}$ (X_C,Y_C) is a cross-point of two lines: a line which is normal to the given line-segment **S** and passes the given point **P** (X_P,Y_P), a line $(y=ax+b)$ extending the given line-segment **S**. If the two endpoints of the line-segment is $\mathbf{E_1}$, $\mathbf{E_2}$, whether the foot of a perpendicular is in the line-segment or not can be determined by the sign of the inner product of two vectors $\mathbf{P_CE_1}$, $\mathbf{P_CE_2}$. Equation (4) shows the equations of the extending line and normal line. Equation (5) shows the equation of cross point $\mathbf{P_C}$ as the solution of above two line equations. Equation (6) defines distance between a point **P** and a line-segment **S**. In this application, the given point **P** is always the camera position and two endpoints of the given line-segment **S** are previously defined $\mathbf{P_{start}}$ and $\mathbf{P_{stop}}$. $\mathbf{P_{start}}$ is nearer to the camera.

$$\begin{cases} y = a \cdot x + b \\ y = -\dfrac{1}{a} \cdot x + \dfrac{1}{a} x_P + y_P \quad \Leftarrow (y - y_P) = -\dfrac{1}{a}(x - x_P) \end{cases} \tag{4}$$

$$P_C(x_C, y_C) = \left(\frac{a}{a^2+1}\left(\frac{1}{a} x_P + y_P + -b\right), \ \frac{a}{a^2+1}\left(x_P + a \cdot y_P + \frac{b}{a}\right) \right) \tag{5}$$

$$\text{distance}(\mathbf{P},\mathbf{S}) \begin{cases} \text{distance}(\mathbf{P},\mathbf{Pc}) & \mathbf{P_CP_{start}} \cdot \mathbf{P_CP_{stop}} < 0 \\ \text{distance}(\mathbf{P},\mathbf{P_{start}}) & \mathbf{P_CP_{start}} \cdot \mathbf{P_CP_{stop}} > 0 \end{cases} \tag{6}$$

$$\mathrm{D}(\mathbf{P},\mathbf{S}) = \text{distance}(\mathbf{P},\mathbf{S}) \times \left(\mathbf{u}(\mathbf{P},\mathbf{P_{start}}) \cdot \mathbf{u}(\mathbf{P_{start}},\mathbf{P_{stop}}) \right) \tag{7}$$

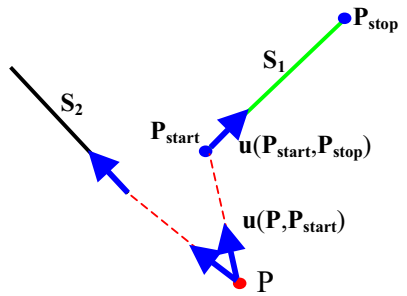

Fig. 8. Guideline is likely to be normal to the gaze

Modified distance D(**P**,**S**) is defined reflecting an assumption that a guideline tends to be normal to the gaze direction. Consequently, modified distance makes guideline detection reliable irrespective of unstable location of start-point $\mathbf{P_{start}}$. How well a marking line-segment is normal to the gaze direction can be measured by the inner product of two unit vectors: a unit vector from the camera position **P** to the start-point $\mathbf{P_{start}}$, $\mathbf{u}(\mathbf{P},\mathbf{P_{start}})$ and a unit vector from the start-point $\mathbf{P_{start}}$ to the stop-point $\mathbf{P_{stop}}$, $\mathbf{u}(\mathbf{P_{start}},\mathbf{P_{stop}})$. Modified distance from a point **P** to a line-segment **S**, D(**P**,**S**), is defined like equation (7) and a line-segment with minimum modified distance is selected as a guideline. Fig. 8 shows the example. Although the start-point of line-segment $\mathbf{S_2}$ is nearer than the start-point of guideline $\mathbf{S_1}$, because the direction of line-segment $\mathbf{S_2}$ is similar to the gaze direction, $\mathbf{S_2}$ has greater modified distance than $\mathbf{S_1}$. Fig. 9 shows the detected guideline.

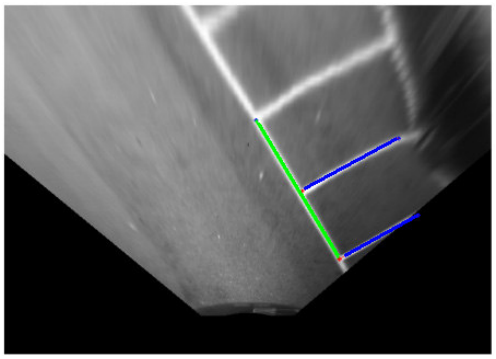

Fig. 9. Recognized guideline

4.2. Dividing Marking Line-Segment

Using the difference between the intensity of pixel on marking and the intensity of pixel off marking along the guideline, marking line-segment dividing parking slots can be detected. Parking slot markings consists of one guideline separating parking slots from roadway and dividing marking line-segments normal to the guideline. By detecting a position where the intensity difference becomes small definitely, 'T'-shape junctions between the guideline and dividing marking line-segments can be recognized successfully. Furthermore, because 'T'-shape junction is searched along a whole line

extending the guideline, additional dividing line-segments, which are not detected during peak pair detection because they are located far and blurred, can be detected.

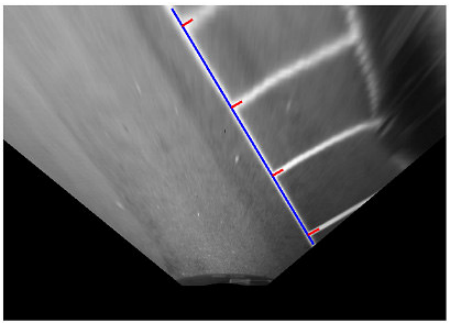

Fig. 10. Recognized dividing marking line-segments

5. Experimental Results

Proposed method for the recognition of parking slot markings successfully operates in the situation when the adjacent slots are occupied by vehicles. Obstacles including adjacent vehicles generate severe distortions in radial manner in bird's eye view image. The reason is that bird's eye view image is constructed using plane surface assumption and obstacle above the ground surface does not satisfy the constraints. In other words, obstacles, which do not belong to the ground surface, will be projected as if it is drawn at the farther location. Especially, bright object among dark background will be stretched long and make a distortion, which can be confused with a marking line-segment. Proposed method alleviates these distortions through 2 phases:

(1) In the edge image of bird's eye view image, marking line-segment appears as a parallel line-segment pair with constant between-distance. Therefore, distortions unsatisfying the constraint will be removed through the peak pair detection in Hough space and the line-segment recognition

(2) If vehicles are normally parked in the adjacent slots beside target free slot, distortions in bird's eye view image caused by these vehicles are supposed to locate beyond the guideline along the perspective direction. Consequently, in spite of the adjacent vehicle's distortion, proposed method can detect the guideline successfully. Once the guideline is recognized correctly, 'T'-shape junction searching can detect dividing marking line-segments and removes the rest noise.

Even if the illumination is too dark and the most portion of parking slot markings are undetectable, guideline tends to appear as a long and distinguishable edge pair. Therefore, guideline can be certainly detected. Once the guideline is recognized, dividing line-segment recognition using weak condition can detect dividing marking line-segments that is missed by the marking line-segment recognition.

(a) Input image

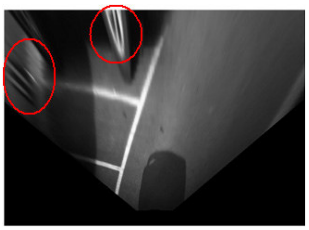

(b) Distortion of adjacent vehicles

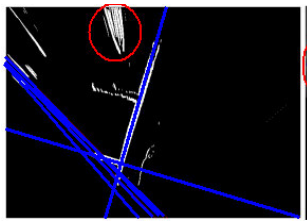

(c) Peak pair detection removes the distortions

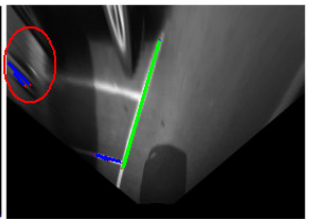

(d) Recognized guideline in spite of mis-detected line-segments

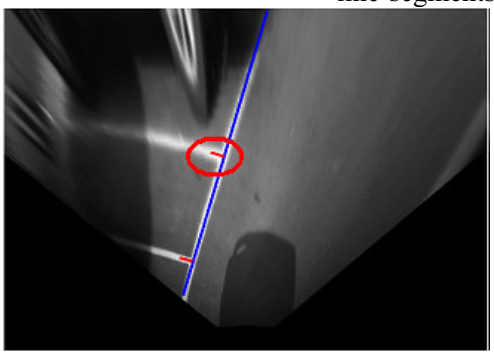

(e) Additionally recognized dividing marking line-segment

Fig. 11. Case study with occlusion by adjacent vehicles

6. Conclusion

This paper proposes a monocular vision system, which recognizes the parking slot markings. Major contributions are marking line-segment recognition using peak pair detection in Hough space and structural pattern recognition of parking slot markings.

References

[1] Richard Bishop, *Intelligent vehicle technology and trends*, Artech Hous Publishers, May 2005, ch. 6.4, ch. 7.1.

[2] Randy Frank, "Sensing in the ultimately safe vehicle", SAE paper no.: 2004-21-0055, Society of Automotive Engineers, 2004.

[3] Masayuki Furutani, "Obstacle detection systems for vehicle safety", SAE paper no.: 2004-21-0057, Society of Automotive Engineers, 2004.

[4] Oliver Bühler, and Joachim Wegener, "Automatic testing of an autonomous parking system using evolutionary computation", SAE paper no.: 2004-01-0459, Society of Automotive Engineers, 2004.

[5] Wei Chia Lee, Werner Uhler, and Torsten Bertram, "Driver centered design of an advanced parking assistance", Proceedings of the 5th European Congress and Exhibition on ITS and Service, 1-3 June 2005.

[6] Asako Hashizume, Shinji Ozawa, and Hirohiko Yanagawa, "An approach to detect vacant parking space in a parallel parking area", Proceedings of the 5th European Congress and Exhibition on ITS and Service, 1-3 June 2005.

[7] Alexander Schanz, Andreas Spieker, and Klaus-Dieter Kuhnert, "Autonomous parking in subterranean garages – a look at the position estimation", Proceedings of the 2003 IEEE Intelligent Vehicle Symposium, 9-11 Jung 2003, pages: 253~258.

[8] C. Vestri, S. Bougnoux, R. Bendahan, K. fintzel, S. Wybo, F. Abad, and T. Kakinami, "Evaluation of a vision-based parking assistance system", Proceedings of the 8th International IEEE Conference on Intelligent Transportation Systems, 13~16 Sep. 2005, pages: 56~60.

[9] K. Fintzel, R. Bendahan, C. Vestri, S. Bougnoux, and T. Kakinami, "3D parking assistant system", Proceedings of the 2004 IEEE Intelligent Vehicle Symposium, 14~17 June 2004, pages: 881~886.

[10] Nico Kaempchen, Uwe Franke, and Rainer Ott, "Stereo vision based pose estimation of parking lots using 3D vehicle models", Proceedings of the 2002 IEEE Intelligent Vehicle Symposium, 17~21 June 2002, pages: 459~464.

[11] Jin Xu, Guang Chen, and Ming Xie, "Vision-guided automatic parking for smart car", Proceedings of the 2000 IEEE Intelligent Vehicle Symposium, 3-5 Oct. 2000, pages: 725~730.

[12] Ho Gi Jung, Dong Suk Kim, Pal Joo Yoon, and Jai Hie Kim, "Stereo vision based localization of free parking site", LNCS Vol. 3691 (CAIP 2005), Sep. 2005, pages: 231~239.

[13] Ho Gi Jung, Dong Suk Kim, Pal Joo Yoon, and Jai Hie Kim, "3D vision system for the recognition of free parking site location", International Journal of Automotive Technology, to be published.

[14] William A. Barrett, and Kevin D. Petersen, "Houghing the Hough: peak collection for detection of corners, junctions and line intersections", Proceedings of the 2001 IEEE Computer Society Conference on Computer Vision and Pattern Recognition (CVPR2001), Vol. 2, 2001, pages: II-302~II-309 vol.2.

[15] Claudio Rosito Jung, and Rodrigo Schramm, "Rectangle detection based on a windowed Hough transform", Proceedins of the XVII Brasilian Symposium on Computer Graphics and Image Processing (SIBGRAPI'04), 17~20 Oct. 2004, pages: 113~120.

[16] Andrew French, Steven Mills, and Tony Pridmore, "Condensation tracking through a Hough space", Proceedings of the 17th International Conference on Pattern Recognition (ICPR'04), 23~24 Aug. 2004, pages: 195~198 vol. 4.

[17] Jean-Yves Bouguet, *Camera Calibration Toolbox for Matlab*, Available: http://www.vision.caltech.edu/bouguetj/calib_doc/index.html.

[18] Ho Gi Jung, Yun Hee Lee, Dong Suk Kim, and Pal Joo Yoon, "Stereo vision based advanced driver assistance system", Proceedings of AVEC International Workshop 2005, 19 Dec. 2005, pages: 97~104.

[19] Yasutaka Furukawa, and Yoshihisa Shinagawa, "Accurate and robust line segment extraction by analyzing distribution around peaks in Hough space", Computer Vision and Image Understanding 92 (2003) pages: 1~25.

[20] Jongwoo Kim, Raghu Krishnapuram, "A robust Hough transform based on validity", Proceedings of the 1998 IEEE World Congress on Computational Intelligence, 4~9 May 1998, pages: 1530~1535 vol.2.